# Data-Driven Model Learning and Control of RCCI Engines based on Heat Release Rate

Radhika Sitaraman\*, Sadaf Batool\*\*, Hoseinali Borhan\*\*\*, Javad Mohammadpour Velni\*\*\*\*, Jeffrey D. Naber<sup>†</sup>, Mahdi Shahbakhti<sup>‡</sup>

\* Cummins Technical Center, Columbus, IN 47201 USA
(e-mail: sitaraman.radhika@cummins.com)

\*\* Michigan Technological University, Houghton, MI 49931 USA
(e-mail: batool@mtu.edu)

\*\*\* Cummins Technical Center, Columbus, IN 47201 USA
(e-mail: hoseinali.borhan@cummins.com)

\*\*\*\* University of Georgia, Athens, GA 30602 USA
(e-mail: javadm@uga.edu)

† Michigan Technological University, Houghton, MI 49931 USA
(e-mail: jnaber@mtu.edu)

‡ University of Alberta, Edmonton, AB Canada
(e-mail: mahdi@ualberta.ca)

**Abstract:** Reactivity controlled compression ignition (RCCI) technology not only offers high thermal efficiency but also produces low nitrogen oxides (NOx) and soot emissions. However, it is imperative to control the combustion in RCCI engines to prevent high pressure rise rates and combustion instability. In this study, a model-based control framework is developed to optimize the RCCI operating mode. To this end, the effects of variations in the premixed ratio, start of injection timing and fuel equivalence ratio on the combustion dynamics are analyzed by examining the heat release rates. Three distinct heat release rate patterns are identified together with two transition zones. Heat release rate traces are grouped together as a function of fractions of early and late heat release rates. Based on a classification algorithm, the fractions of early and late heat release rate are identified as scheduling variables for the data-driven modeling of an RCCI engine. Linear regression is used to model the fractions of early and late heat release. These models are then used to train linear parameter varying (LPV) models using least-squares support vector machine (LS-SVM). Using the learned LPV model, a model predictive controller (MPC) scheme is then developed for a 2-liter 4-cylinder RCCI engine to control combustion phasing (CA50) and indicated mean effective pressure (IMEP) while limiting the maximum pressure rise rate (MPRR) to avoid engine knocking. The simulation results show that the designed controller is capable of limiting MPRR below 6 bar/CAD while tracking CA50 and IMEP with average errors of 1.2 CAD and 6.2 kPa, respectively.

Keywords: Machine Learning; Support Vector Machines (SVM); Model Predictive Control (MPC); Multi-input Multi-output Control; Reactivity Controlled Compression Ignition (RCCI)

#### 1. INTRODUCTION

Low temperature combustion (LTC) modes are among the advanced combustion technologies that offer high thermal efficiency and ultra-low NOx and soot emissions. NOx is formed when the diffusion flame front comes in contact with the premixed charge (Dec, 1997). However, soot formation is associated with the fuel rich zones of the fuel plume (Dec, 1997). Furthermore, NOx is formed at

high combustion temperatures usually > 2200 K while the combustion temperatures are mostly in the range of 1400-2100 K in LTC engine (Maurya, 2018). In an LTC engine, combustion temperatures are usually low (Hanson and Reitz, 2015). In addition, Soot formation is prevented by highly premixed and lean air-fuel mixtures while NOx formation is prevented by having a premixed volumetric combustion (Agarwal et al., 2017). Multiple concepts of LTC and their combustion control are demonstrated by researchers (Agarwal et al., 2017; Shaver et al., 2009; Ravi et al., 2006; Hellstrom et al., 2014; Zhang et al., 2014; Hanson and Reitz, 2015; Batool et al., 2022) using either single fuel or a combination of two fuels.

 $<sup>^\</sup>star$  This work is supported by the United States National Science Foundation (awards #1762520 and #1762595) and the U.S Department of State, Bureau of Educational and Cultural Affairs, Fulbright Program.

Reactivity controlled compression ignition (RCCI) is among the LTC modes in which combustion is attributed to the reactivity gradient of the dual fuels. When compared with homogeneous charge compression ignition (HCCI), RCCI mode provides additional control levers such as difference in reactivity of both fuels, start of injection timing of the higher reactivity fuel and the ratio of both low reactivity and high reactivity fuels for combustion control (Dempsey, 2013; Kokjohn et al., 2011; Paykani et al., 2016). Due to premixed air-fuel mixtures in the LTC modes, the auto-ignition of air-fuel mixture usually results in very high maximum pressure rise rates (MPRR) which can cause engine knocking. However, through optimal control of injection timing of high reactivity fuel and premixed ratio, high MPRR can be prevented. Model-based control of RCCI mode can be utilized for safe engine operation while ensuring optimal engine operation. Control oriented models (COMs) suitable for controller design are categorized as either physics-based engine models or data-driven models. The physics-based engine models can be calibrated using experimental data, which is time consuming. As an alternative, data driven approaches have gained significance. In data driven approaches, the relationship between inputs and outputs of the system is modeled, without complex physics based modeling of the system (Solomatine

Various combustion metrics such as heat release rate (HRR), start of combustion (SOC), combustion phasing (CA50), burn duration (BD), indicated mean effective pressure (IMEP), maximum pressure rise rate (MPRR), and coefficient of variation of indicated mean effective pressure  $(COV_{IMEP})$  can be analyzed with machine learning techniques. Multiple machine learning techniques have been explored to build engine models that are compatible for internal combustion engines (ICEs) controls. Machine learning algorithms used to model LTC engine include feedforward neural network (FFNN) (Rezaei et al., 2015), radial basis function neural network (RBFNN) (Rezaei et al., 2015; Wong et al., 2013), artificial neural network (ANN) Bidarvatan and Shahbakhti (2014); Roy et al. (2014), kernel based extreme learning machine (ELM) (Wong et al., 2015, 2013), least-squares support vector machine (LS-SVM) (Wong et al., 2013; Irdmousa et al., 2019; Rizvi et al., 2015), and support vector machines (SVM) classification algorithms (Batool et al., 2021). Early and high rate of heat release can cause high pressure rise rates while late heat release can result in incomplete combustion. In addition, optimum heat release shape enables an RCCI engine to obtain the maximum brake thermal efficiency. Therefore, this study is based on control of RCCI mode for optimal engine operation by controlling the rate of heat release. This is achieved by developing an RCCI engine model as a function of fractions of early and late heat release for the control of CA50 (crank angle where 50% heat is released) and IMEP while limiting MPRR.

To the best of the authors' knowledge, this is the first study undertaken to develop a learning based engine model based on the heat release types to control the combustion in an RCCI engine. Linear parameter varying (LPV) models are developed using support vector machines (SVM). This learning-based model is used to develop an MPC scheme for a 4-cylinder RCCI engine to control load and CA50

while limiting MPRR. The main contributions of this work include:

- (1) Modeling of fractions of early and late heat release using multivariable regression to represent different types of heat release rates;
- (2) Development of control-oriented linear parameter varying (LPV) models as a function of fractions of early and late heat release. Least-square support vector machine (LS-SVM) is used to train the LPV models;
- (3) Development of an MPC framework based on the LPV models for RCCI combustion to control CA50 and IMEP while limiting MPRR;
- (4) Validation of disturbance rejection performance of the controller in the presence of measurement uncertainty to track CA50 and IMEP while limiting MPRR.

The organization of paper is as follows: Section 2 includes the experimental setup and the range of data collected. Section 3 explains the different types of heat release rates observed in RCCI engine. Section 4 provides the details about the modeling of RCCI engine using lease square support vector machines algorithm. Section 5 describes the model predictive control framework. Results and discussions are provided in section 6. Section 7 summarizes the major findings of this work.

# 2. EXPERIMENTAL SETUP AND DATA COLLECTION

In this study, a 2.0L, 4-cylinder gasoline direct injection GM engine coupled with a 460hp AC dynamometer was used. Two port-fuel injection (PFI) systems were appended to the original engine. The engine was calibrated using a prototype engine control unit (ECU). Figure 1 shows the experimental setup of the RCCI engine used in this study. RCCI engine operation was achieved at wide open throttle under naturally aspirated conditions without exhaust gas recirculation (EGR). The intake air was preheated to the required temperature using a controlled air-heater. PCB piezoelectric pressure transducer with a resolution of 1 CAD was used to measure the in-cylinder gas pressure. A dSPACE MicroAutoBox (MABX) and a Xilinx Spartan-6 field programmable gate array (FPGA) were used as the engine control unit and for the real time feedback of combustion parameters, respectively. The detailed engine instrumentation can be found in Kannan (2016).

In the RCCI mode, port fuel injectors were used for the injection of iso-octane during intake stroke, and direct injectors were used for the injection of n-heptane during the compression stroke. The premixed ratio of the two fuels is determined using

$$PR = \frac{m_{\rm iso}LHV_{\rm iso}}{m_{\rm iso}LHV_{\rm iso} + m_{\rm nhep}LHV_{\rm nhep}}$$
(1)

where,  $m_{\rm iso}$  and  $m_{\rm nhep}$  are the masses of iso-octane and n-heptane, respectively. LHV<sub>iso</sub> and LHV<sub>nhep</sub> represent the lower heating values of iso-octane and n-heptane, respectively.

The engine data was recorded for 100 consecutive cycles at different steady state operating conditions. The range

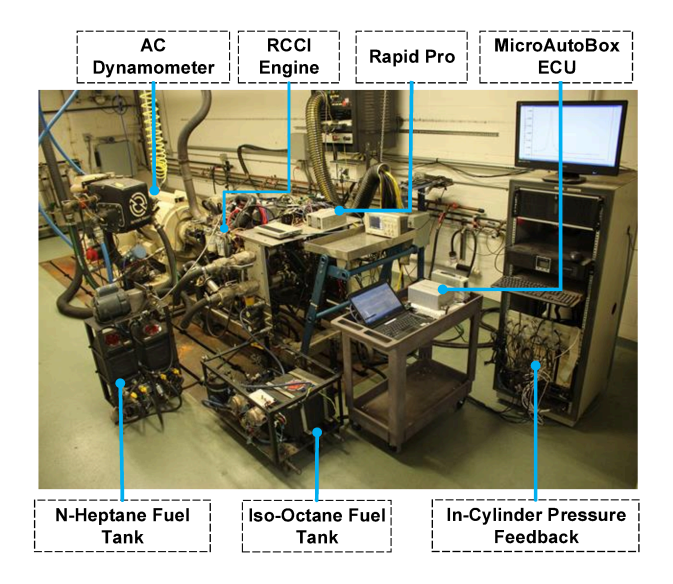


Fig. 1. Experimental setup used in this study, where the engine operates at the RCCI mode.

of operating conditions of the RCCI engine data used in this study is shown in Table 1.

Table 1. Operating range of RCCI engine operation

Parameters	Range
Engine speed, N (RPM)	800-2,300
Intake temperature, T <sub>man</sub> (°C)	40-100
Manifold pressure, P <sub>man</sub> (kPa)	96
Start of injection, SOI (CAD bTDC)	15-100
Premixed ratio, PR (-)	20-60
Fuel quantity, FQ (mg/cyc)	9-40

# 3. DATA-DRIVEN MODELING OF RCCI

Based on the shape, three different heat release rate patterns were observed in RCCI engine operation. Rule based classification of heat release rate traces was carried out based on the subject knowledge. The classified data form the basis for developing a supervised machine learning control oriented model. In order to classify the data, the crank angles at the start and end of main heat release were identified and logged manually for each of the HRR traces, as shown in Fig. 2.

The percentage of heat released before the main stage combustion event was calculated based on the crank angles associated with the start of injection (SOI) and the start of main heat release (SOM). This percentage of heat release is termed as fraction of early heat release ( $HR_{early}$ ). Similarly, the percentage of heat release between the crank angle of the end of main stage heat release (EOM) and the crank angle corresponding to 90% of heat release (CA90) are calculated. This percentage of heat release is termed as fraction of late heat release ( $HR_{late}$ ). Fractions of early and late heat release are determined using (2) and (3), respectively.

$$HR_{early} = \frac{Cumulative \ HR \mid_{SOI}^{SOM}}{\text{Energy in the injected fuel}} \times 100$$
 (2)

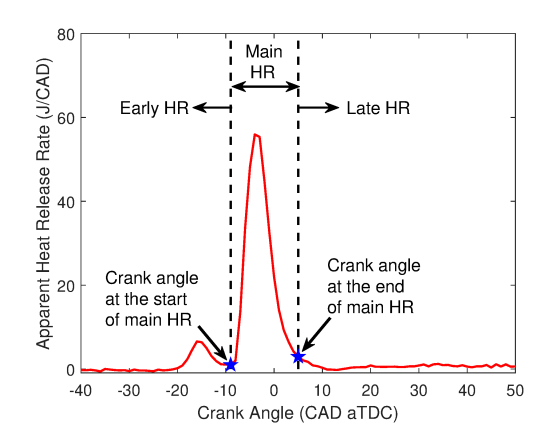


Fig. 2. Heat release rate trace with start and end of main heat release (HR) depicted

$$HR_{late} = \frac{Cumulative~HR\mid_{EOM}^{CA90}}{\text{Energy in the fuel quantity injected}} \times 100~~(3)$$

The HRR traces are classified based on the fraction of early and late heat release values. Using decision trees, complete classification is achieved. The threshold values for different types of heat release rate were determined by analyzing the experimental data. If the fraction of early heat release is  $\leq 5\%$  and the fraction of late heat release is < 17%, then the HRR is classified as Type-1. If the fraction of early heat release is > 7%, then the HRR is classified as Type-2. If the fraction of early heat release is  $\leq 5\%$  and the fraction of late heat release is  $\geq 23\%$ , then the HRR is classified as Type-3. If the fraction of early heat release is  $\leq 5\%$  and the fraction of late heat release is  $\geq 17\%$  but < 23%, then the HRR is classified as Type-4. If the fraction of early heat release is > 5% but < 7%, then the HRR is classified as Type-5.

Summarized are few traces from each classification type in Fig. 3, depicting 3 classification bins. In addition to these three basic types, two more HR shapes were identified as Type-4 and Type-5 which represented the combustion phase transition between the three HRR types shown in Fig. 3. Summary of the count of HRR traces identified into

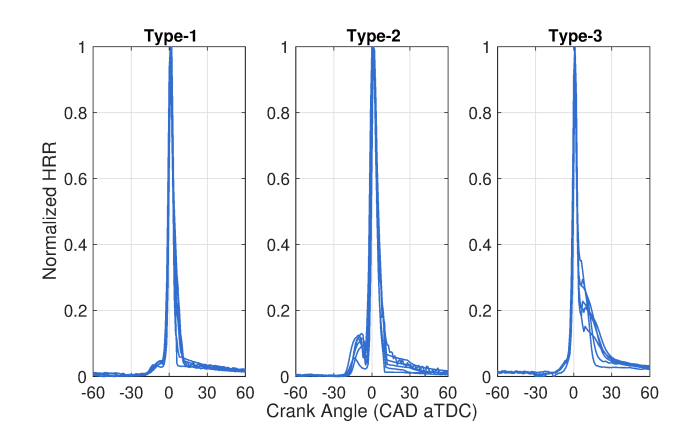


Fig. 3. Sample heat release rate traces for three main HRR patterns

each type is listed in Table 2.

Table 2. Summary of the classified HRR traces

Type of HRR traces	Count of traces
Type 1	131
Type 2	71
Type 3	373

In RCCI engine, heat release rate pattern changes with change in the operating conditions, i.e., engine speed, intake manifold pressure and temperature and manipulated variables (fuel quantity, SOI and PR). Hence, it is evident that heat release pattern variation is a multi-dimensional data frame. To model complex heat release in the RCCI engine, we used linear parameter varying (LPV) state-space representation to capture nonlinear engine behavior. This LPV state-space model is then used for combustion control. Thus, we need to identify the scheduling parameters for the LPV model that can represent the nonlinearity of the RCCI engine. With proper selection of a scheduling variables, details of change in HRR pattern of the engine can be decoded. Fractions of early and late HR are identified as scheduling variables for the LPV modeling of the engine.

Multi-variable linear regression technique is used to model the scheduling variables. For a model with p explanatory variables,  $x_1, x_2, x_3, ..., x_p$  and y as response variable, the model is represented as

$$y_i = \beta_0 + \beta_1 x_{i_1} + \beta_2 x_{i_2} + \dots + \beta_p x_{i_p} + \epsilon_i$$
 (4)

where n is the number of observations and i=1,2,3,...,n. The model fitting is governed by the coefficients  $(\beta_0, \beta_1, \beta_2,..., \beta_p)$  of the explanatory variables and  $\epsilon$  depicts the residual term.

The best line fitting data was evaluated by using a cost function. Cost function is a sum of squares of vertical distance from each data point to the predicted value by the fitted line divided by number of observations. The cost function is described in terms of mean square error (MSE). By minimizing the cost function, the coefficients of the best fit line were determined. Start of injection, premixed ratio, fuel quantity and engine speed were selected as input parameters to model the fractions of early and late HR using regression. Multiple combinations were evaluated to model fractions of early and late HR and the accuracy of different models was compared on the basis of the R-square value. Upon evaluating different regression models, two functions with the best  $R^2$  were determined

$$HR_{early} = f(SOI, PR, FQ, N),$$
 (5)

$$HR_{late} = g(SOI, PR, FQ, N).$$
 (6)

The  $R^2$  value of fraction of early heat release is 69.6 while the  $R^2$  value of fraction of late heat release is 80.4. The identified combustion classifiers are used as scheduling parameters to build an LPV model of the RCCI engine. By using combustion classifiers as scheduling variables for the LPV models, the information of combustion type is incorporated into RCCI engine model. LS-SVM is then used for identification of an LPV model as a function of fractions of early and late heat release. The classification

of heat release types with experimental values of fraction of early HR and fraction of late HR is shown in Fig. 4.

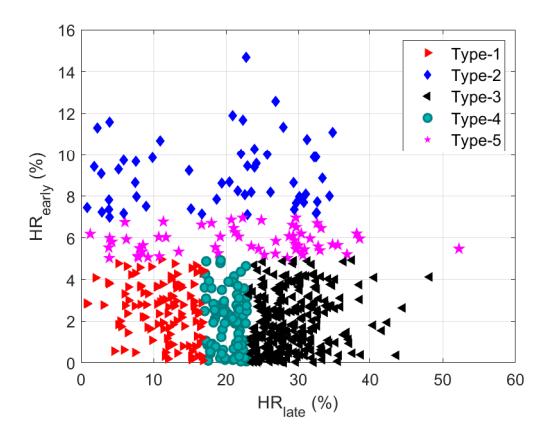


Fig. 4. Classification of experimental data based on fractions of early and late HR

#### 4. LS-SVM FOR LPV MODEL LEARNING

SVM regression approach is used to identify the state space matrices of the engine model in the LPV framework. Following state-space representation is considered

$$X_{k+1} = A(p_k)X_k + B(p_k)U_k + K(p_k)e_k$$
  

$$Y_k = C(p_k)X_k + D(p_k)U_k + e_k$$
(7)

where X represents states of the system, Y is the measurable output, U is the control input, p represents the scheduling parameter, and e represents stochastic white noise.  $A(p_k)$ ,  $B(p_k)$ ,  $C(p_k)$ ,  $D(p_k)$  and  $K(p_k)$  represent the state space matrices of the system which vary as a function of the parameter  $p_k$ . Equation (7) is restructured as

$$e_k = Y_k - C(p_k)X_k - D(p_k)U_k. \tag{8}$$

Eq. (7) can be rewritten as follows by substituting  $e_k$ :

$$X_{k+1} = \bar{A}(p_k)X_k + \bar{B}(p_k)U_k + K(p_k)Y_k$$

$$Y_k = C(p_k)X_k + D(p_k)U_k + e_k$$
(9)

where

$$\bar{A} = A(p_k) - K(p_k)C(p_k),$$

$$\bar{B} = B(p_k) - K(p_k)D(p_k).$$
(10)

The plant matrices  $\bar{A}(p_k)$ ,  $\bar{B}(p_k)$ ,  $C(p_k)$ ,  $D(p_k)$  and  $K(p_k)$  are computed using support vector machine approach. By taking the training data into SVM framework, the plant matrices are transformed using weighing matrices (W), regression vectors or features  $(\phi)$ .

Following is obtained by representing the regression vector  $(\phi)$  as a function of basis function  $(\Phi)$ 

$$X_{k+1} = W_1 \Phi_1(p_k) X_k + W_2 \Phi_2(p_k) U_k + W_3 \Phi_3(p_k) Y_k + \epsilon_k$$
$$Y_k = W_4 \Phi_4(p_k) X_k + W_5 \Phi_5(p_k) U_k + \zeta_k,$$
(11)

where  $\epsilon$  and  $\zeta$  represent the residual error. Details on the learning of the LPV model can be found in (Rizvi et al., 2015).

Transient engine data is required to identify the state space LPV model. Transient engine data was collected from the experimentally validated RCCI engine model (Raut, 2017;

Basina et al., 2020) by varying operating conditions and the control inputs to the engine as shown in Fig. 5. SOI of the DI fuel, FQ and PR are the engine manipulated variables changed during the test. Engine speed was kept constant at 1000 rpm.

## 4.1 RCCI Engine Modeling

Using the LS-SVM approach, combustion parameters are predicted by developing the state space LPV model. States of the system (X) are:

$$X = \begin{bmatrix} CA50 & MPRR & T_{soc} & P_{soc} & IMEP \end{bmatrix}^T, \qquad (12)$$

where  $T_{soc}$  and  $P_{soc}$  are the temperature and pressure at start of combustion. Manipulated Variables of the system (U) are:

$$U = \begin{bmatrix} SOI & FQ & PR \end{bmatrix}^T. \tag{13}$$

Scheduling parameters of the system (p) are:

$$P = \begin{bmatrix} p_1 & p_2 \end{bmatrix}^T, \tag{14}$$

where  $p_1$  is the fraction of early HR and  $p_2$  is the fraction of late HR. Output of the system (Y) is:

$$Y = \begin{bmatrix} CA50 & MPRR & IMEP \end{bmatrix}^T. \tag{15}$$

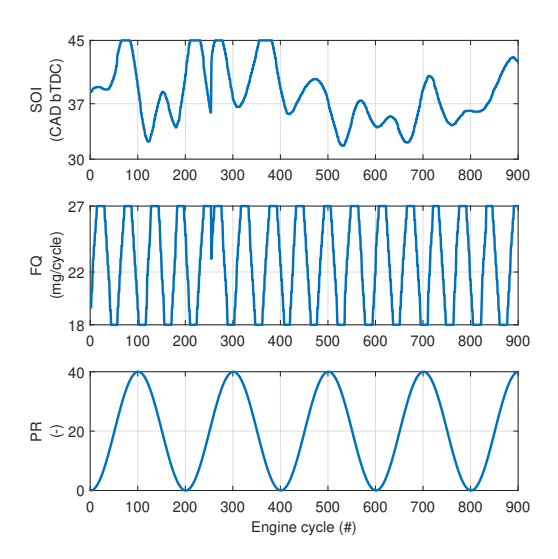


Fig. 5. Manipulated variables of the RCCI engine at N = 1000 RPM,  $T_{man} = 333$  K and  $P_{man} = 96.5$  kPa.

Figure 5 shows the manipulated variables of the RCCI engine. The range of manipulated variables also defines the range of the training data set used for the RCCI engine model. Furthermore, the input parameters are varied such that the data covers all the HR types.

In Fig. 6, the comparison of prediction and measured values of the RCCI engine is shown. 35% of the data used for testing is shown in the plot. The LPV model is able to predict CA50, MPRR and IMEP with RMSE of 0.4 CAD, 0.5 bar/CAD and 9.6 kPa, respectively.

### 5. MODEL PREDICTIVE CONTROL DESIGN

An MPC controller is designed for combustion control of the RCCI engine. The MPC framework is developed

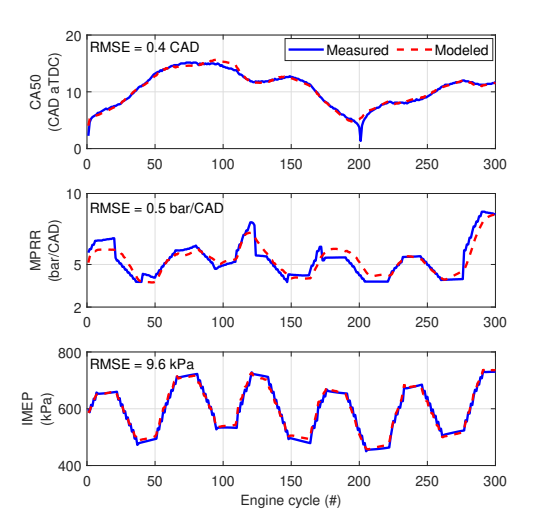


Fig. 6. Comparison of measured and modelled output of the RCCI engine at N = 1000 RPM,  $T_man = 333$  K and  $P_man = 96.5$  kPa

based on the LPV model to predict future outputs and optimize the manipulated variables based on the defined cost function. During the RCCI engine operation, the system matrices at any instant are derived as a function of  $p_1$  (fraction of early HR) and  $p_2$  (fraction of late HR). Prediction of states and outputs of the optimization problem is achieved for certain future time steps. The control horizon and prediction horizon are selected as 20 and 10 engine cycles, respectively.

A quadratic problem (QP) is developed which is optimized for the identification of manipulated variables of the system. Constraints on manipulated variables, their rate of change, states and outputs of the system are added. Cost function of the optimization problem is defined as the sum of three terms in the current design as

$$J(z_k) = J_y(z_k) + J_{\Delta u}(z_k) + J_{\epsilon}(z_k), \tag{16}$$

where  $z_k$  is the QP decision variable over the control interval, k is the current control interval,  $J_y$  refers to output reference tracking,  $J_{\Delta u}$  refers to manipulated variable tracking, and  $J_{\epsilon}$  refers to constraint violation. Output reference tracking is achieved by the controller cost as

$$J_{y}(z_{k}) = \sum_{j=1}^{n_{y}} \sum_{i=1}^{p} \left\{ \frac{w_{i,j}^{y}}{s_{j}^{y}} \left[ r_{j}(k+i|k) - y_{j}(k+i|k) \right] \right\}^{2}, \quad (17)$$

in which p represents the prediction horizon,  $\mathbf{n}_y$  refers to the number of plant outputs,  $\mathbf{z}_k$  is the decision variable of the QP as

$$z_k^T = [u(k|k)^T \quad u(k+1|k)^T \quad u(k+p-1|k)^T \quad \epsilon_k],$$
(18)

and  $\mathbf{r}_j(k+i|k)$  and  $\mathbf{y}_j(k+i|k)$  denote the reference and predicted value of the j<sup>th</sup> plant output at the i<sup>th</sup> step of the prediction horizon, respectively. Furthermore,  $s_j^y$  refers to the scale factor for the j<sup>th</sup> plant output and  $\mathbf{w}_{i,j}^y$  is the tuning weight for the j<sup>th</sup> plant output at the i<sup>th</sup> step of the prediction horizon.

The second term in the cost function that keeps the rate of change of manipulated variables of the system is:

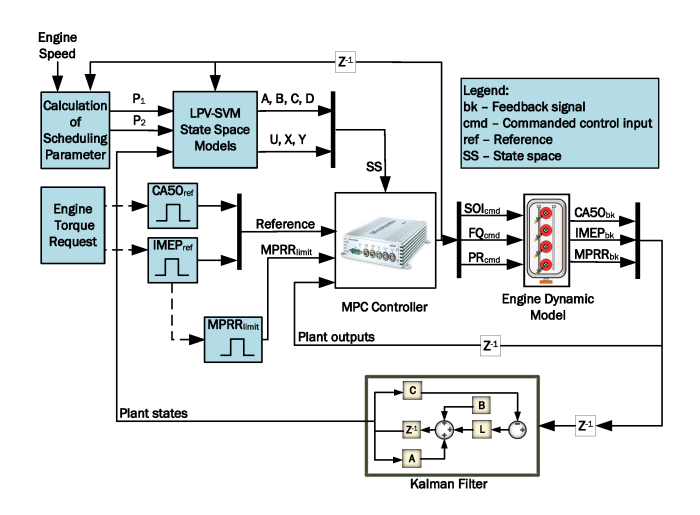


Fig. 7. Schematic of the designed LPV-MPC controller for the RCCI engine

Table 3. Summary of constraints applied on manipulated variables and outputs of the adaptive MPC

Variable	Minimum constraint	Maximum constraint
SOI (CAD bTDC)	32	45
FQ (mg/cycle)	18	27
PR (-)	0	40
CA50 (CAĎ aTDC)	-10	30
IMEP (kPa)	500	1000
MPRR (bar/CAD)	0	6

$$J_{\Delta u}(z_k) = \sum_{j=1}^{n_u} \sum_{i=0}^{p-1} \left\{ \frac{w_{i,j}^{\Delta u}}{s_j^u} \left[ u_j(k+i|k) - u_{jtarget}(k+i|k)) \right] \right\}^2,$$
(19)

where  $n_u$  refers to the number of manipulated variables,  $s_j^u$  refers to the scaling factor for the  $j^{th}$  plant output and  $w_{i,j}^{\Delta u}$  is the tuning weight for the  $j^{th}$  plant manipulated variable rate of change at the  $i^{th}$  step of the prediction horizon.

The designed controller employs the term  $J_{\epsilon}$  to measure the violation of constraints as

$$J_{\epsilon}(z_k) = \rho_{\epsilon} \epsilon_k^2, \tag{20}$$

where  $\epsilon_k$  is the slack variable at control interval k, and  $\rho$  represents the penalty weight associated with it. The maximum and minimum limit set on the plant outputs, manipulated variables and the rate of change of manipulated variables predominantly constitute the explicit constraints associated with the MPC. The upper and lower bounds of the constraints applied are presented in Table 3.

# 6. RESULTS AND DISCUSSIONS

Control structure of the designed MPC controller is shown in Fig. 7. MPC is used to track the outputs, CA50 and IMEP of the system and to limit MPRR by using SOI, fuel quantity and PR as manipulated variables. Physics-based engine model is used as the plant (Raut, 2017). The weights of the allowed rate of change of manipulated variables and output are tuned to achieve required tracking performance. A Kalman filter is used to

predict the unmeasured states of the engine. The CA50 and IMEP reference trajectories are determined from the engine speed and the torque request to the engine electronic control module.

Fig. 8 shows the tracking performance of the designed controller. The desired reference trajectories for CA50 and IMEP were changed from 5 to 12 CAD aTDC and IMEP from 525 kPa to 650 kPa, respectively. The system tracked the change in outputs by keeping MPRR less than 6 bar/CAD. The changes in manipulated variables and scheduling parameter of the LPV system were also evaluated in the various cases.

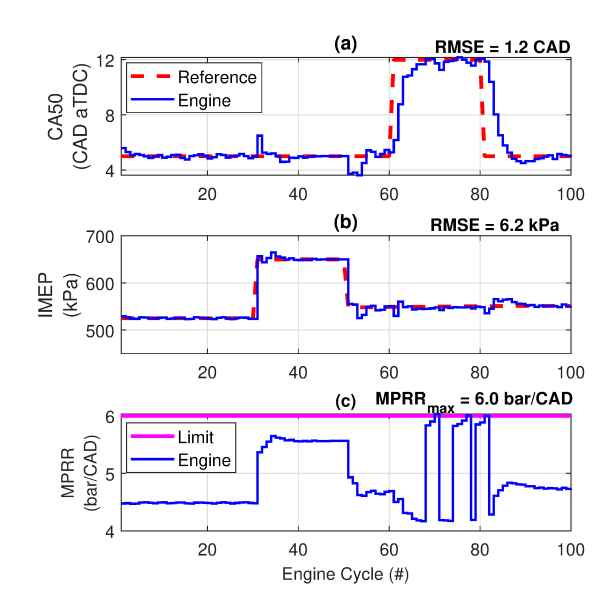


Fig. 8. Tracking capability of the designed controller to follow desired CA50 and IMEP with the MPRR limit of 6 bar/CAD

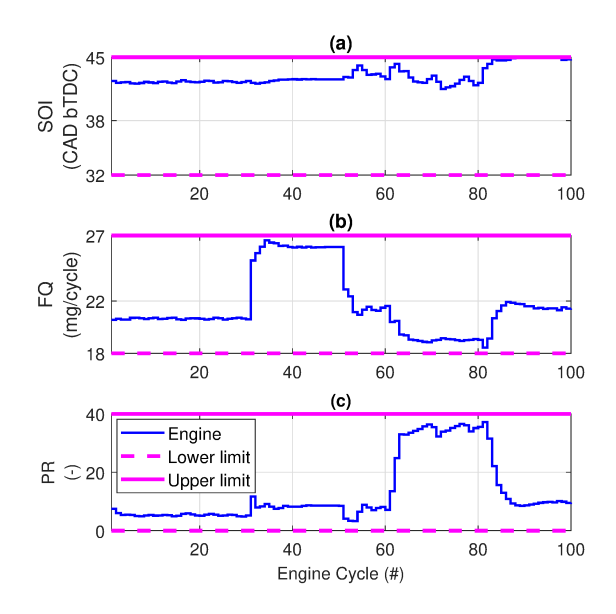


Fig. 9. Controller action to follow desired CA50 and IMEP with the MPRR limit of 6 bar/CAD

In Fig. 8, the tracking ability of designed controller to follow the desired change in both CA50 and IMEP was eval-

uated. Controller was able to track CA50 and IMEP with RMSE of 1.2 CAD and 6.2 kPa while limiting MPRR to 6 bar/CAD. The controller showed faster IMEP tracking for a step change while a slower response for a step change in CA50 was observed. The slow CA50 tracking response can be mainly attributed to the controller action responsible to keep the MPRR below the set limit. However, the CA50 response can be improved by relaxing the constraint on MPRR to a higher value (e.g., 8 bar/CAD). Figure 9 shows the controller action for tracking CA50 and IMEP while limiting MPRR. The control actions stay within the set constraints. Figure 10 represents the fractions of early HR (P1) and late HR (P2) representing different types of heat release rates resulting from the control actions. The fractions of early and late HR are the scheduling parameters for the LPV state space models. For the first 30 engine cycles,  $HR_{early}$  is between 5-7% which means the resulting heat release rate is type-5. When the desired IMEP changes to 650 kPa, the resulting control actions lead to type-1 heat release rate with  $HR_{early} < 5\%$  and  $HR_{late} < 17\%$ . When there is a step change in desired CA50 at  $60^{th}$  engine cycle,  $HR_{early}$  becomes < 5% while  $HR_{late}$  is  $\geq 17\%$  and < 23%, resulting in type-4 heat release

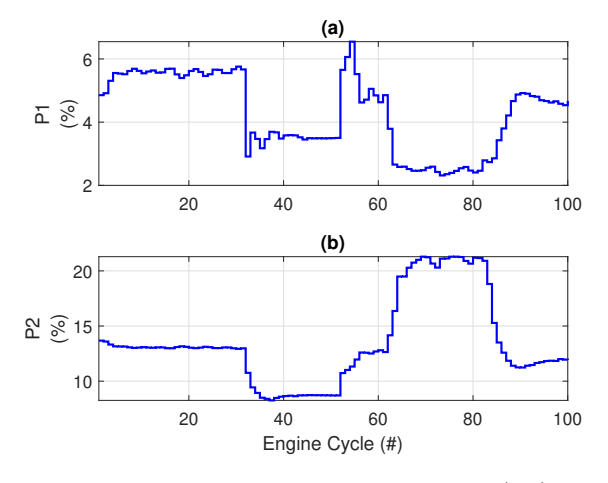


Fig. 10. Variation in fractions of early HR (P1) and late HR (P2) while tracking desired CA50 and IMEP with the MPRR limit of 6 bar/CAD

Figure 11 shows the tracking capability of the designed controller for the RCCI engine in the presence of measurement uncertainties. The measurement uncertainties were added to the outputs of the physics-based engine model. Based on the actual experimental data, the measurement uncertainty of  $\pm 1$  CAD,  $\pm 28.1$  kPa and  $\pm 0.6$  bar/CAD were added to CA50, IMEP and MPRR, respectively. Tracking with RMSE of 2.2 CAD for CA50, RMSE of 17.3 kPa for IMEP and the maximum pressure rise rate is observed to be 6.4 bar/CAD. Error in tracking had gone up due to uncertainty in the outputs. In  $83^{rd}$  engine cycle, a violation in the MPRR constraint was observed because of the saturation of the manipulated variables as shown in Fig. 12. The controller comes into action to bring the MPRR within the desired limit in subsequent cycles.

#### 7. SUMMARY AND CONCLUSION

In this research work, a control-oriented model of an RCCI engine is developed based on different heat release

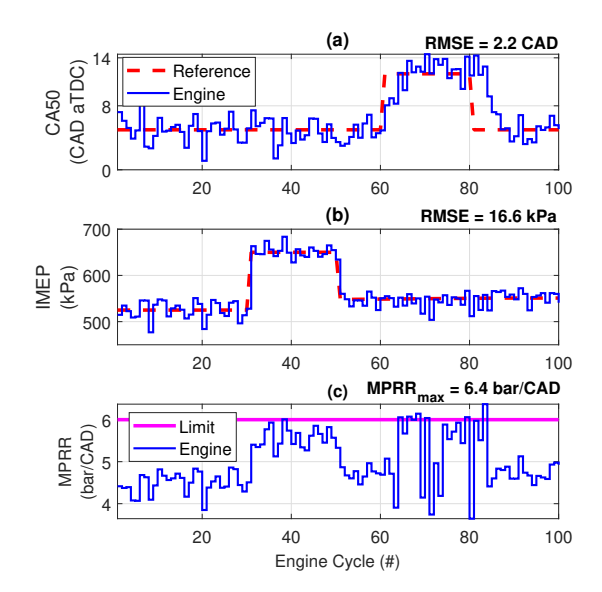


Fig. 11. Tracking capability of the designed controller under measurement uncertainty of  $\pm 1$  CAD,  $\pm 28.1$  kPa and  $\pm 0.7$  bar/CAD added to the measured outputs of the RCCI engine model.

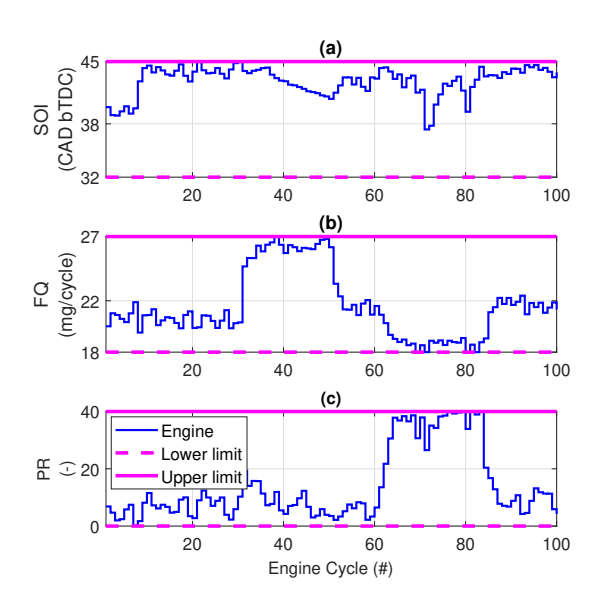


Fig. 12. Tracking capability of the designed controller under measurement uncertainty of  $\pm 1$  CAD,  $\pm 28.1$  kPa and  $\pm 0.6$  bar/CAD added to the measured outputs of the RCCI engine model.

rate shapes. Major engine inputs leading to different heat release shapes were identified. The parameters including fraction of early heat release and fraction of late heat release were used as scheduling variables to obtain an linear parameter varying representation of the RCCI engine in state-space domain using kernel-based system identification method. A multi-input multi-output MPC framework is designed to control the CA50 and IMEP while limiting MPRR below 6 bar/CAD. A summary of findings includes:

• Using Support Vector Machine (SVM) approach, an LPV model representation for the RCCI engine was learned. The model was validated with the data gen-

- erated by the detailed RCCI engine dynamic model. It was able to predict CA50, IMEP and MPRR with RMSE of 0.4 CAD, 16.6 kPa and 0.4 bar/CAD, respectively.
- The controller was able to track CA50 and IMEP with MPRR constraint of 6 bar/CAD with SOI, PR and fuel quantity as manipulated variables. It was able to track CA50 and IMEP with RMSE of 1.2 CAD and 6.2 kPa, respectively.
- Robustness of the MPC was also evaluated by the addition of measurement uncertainties to the outputs of the detailed physics-based dynamic engine model. The MPC controller was able to track CA50 and IMEP with RMSE of 2.2 CAD and 17.3 kPa with a constraint of 6 bar/CAD on MPRR.

Future work includes testing of the designed controller on the actual engine setup.

#### REFERENCES

- Agarwal, A., Singh, A., and Maurya, R. (2017). "Evolution, challenges and path forward for Low temperature combustion". *Progress in Energy and Combustion Science*, 61, 1–56.
- Basina, L.N.A., Irdmousa, B.K., Velni, J.M., Borhan, H., Naber, J.D., and Shahbakhti, M. (2020). "Data-driven Modeling and Predictive Control of Maximum Pressure Rise Rate in RCCI Engines". In 2020 IEEE Conf. on Cont. Tech. and App. (CCTA), 94–99.
- Batool, S., Naber, J.D., and Shahbakhti, M. (2021). "Data-Driven Modeling and Control of Cyclic Variability of an Engine Operating in Low Temperature Combustion Modes". *IFAC Mod.*, Est. and Cont. Conf. (MECC).
- Batool, S., Naber, J.D., and Shahbakhti, M. (2022). "Multi-mode Low Temperature Combustion (LTC) and Mode Switching Control". In Agarwal A.K., Martinez A.G., Kalwar A., Valera H. (eds). Advanced Combustion for Sustainable Transport, Energy, Environment, and Sustainability, 43–93. Springer, Singapore.
- Bidarvatan, M. and Shahbakhti, M. (2014). "Gray-box modeling for performance control of an HCCI engine with blended fuels". *Journal of Engineering for Gas Turbines and Power*, 136.
- Dec, J. (1997). "A Conceptual Model of DI Diesel Combustion Based on Laser-Sheet Imaging". In *SAE Technical Paper*. SAE International. 970873.
- Dempsey, A. (2013). "Dual Fuel Reactivity Controlled Compression Ignition(RCCI) with Alternative Fuels". Ph.D. thesis, University of Wisconsin-Madison.
- Hanson, R. and Reitz, R. (2015). "Investigation of Cold Starting and Combustion Mode Switching as Methods to Improve Low Load RCCI Operation". In *Proc. of the ASME 2015 Int. Comb. Eng. Div. Fall Tech. Conf.* Adv. Comb., USA.
- Hellstrom, E., Larimore, J., Jade, S., Stefanopoulou, A.G., and Jiang, L. (2014). "Reducing Cyclic Variability While Regulating Combustion Phasing in a Four-Cylinder HCCI Engine". *IEEE Trans. on Cont. Sys. Tech.*, 22(3), 1190–1197.
- Irdmousa, B., Rizvi, S., Velni, J., Naber, J., and Shah-bakhti, M. (2019). "Data Driven Modelling and Predictive Control of Combustion Phasing for RCCI Engines".

- In 2019 American Control Conference (ACC), 1617–1622.
- Kannan, K. (2016). "An experimental investigation of Low temperature Combustion regimes in a light duty". Master's thesis, Michigan technological University.
- Kokjohn, S., Hanson, R., Splitter, D., and Reitz, R. (2011). "Fuel reactivity Controlled Compression Ignition (RCCI):A pathway to Controlled High Efficiency Clean Combustion". *International Journal of Engine Research*, 12, 209–226.
- Maurya, R.K. (2018). "Multi-mode Low Temperature Combustion (LTC) and Mode Switching Control". In *Low Temperature Combustion Engines*, 31–133. Springer, Cham.
- Paykani, A., Kakaee, A., Rahnama, P., and Reitz, R. (2016). "Progress and recent trends in Reactivity controlled compression Ignition Engines". *International Journal of Engine Research*, 17, 481–524.
- Raut, A. (2017). "Model based control of RCCI Engine". Master's thesis, Michigan technological University.
- Ravi, N., Roelle, M.J., Jungkunz, A.F., and Gerdes, J.C. (2006). "A Physically Based Two-State Model for Controlling Exhaust Recompression HCCI in Gasoline Engines". Proc. of the ASME 2006 Int. Mech. Engg. Congress and Expo. Dyn. Sys. and Cont., Parts A and B., pp. 483–492.
- Rezaei, J., Shahbakhti, M., Bahri, B., and Aziz, A. (2015). "Performance prediction of HCCI engines with oxygenated fuels using artificial neural networks". *Applied Energy*, 138, 460 473.
- Rizvi, S., Velni, J., Toth, R., and Meskin, N. (2015). "A Kernel based Approach to MIMO LPV State Space Identification and Application to a Nonlinear Process System". *IFAC-PapersOnLine*, 48, 85 90. 1st IFAC Workshop on Linear Parameter Varying Systems LPVS 2015
- Roy, S., Banerjee, R., and Bose, P. (2014). "Performance and exhaust emissions prediction of a CRDI assisted single cylinder diesel engine coupled with EGR using artificial neural network". *Applied Energy*, 119, 330 340.
- Shaver, G.M., Gerdes, J.C., and Roelle, M.J. (2009). "Physics-Based Modeling and Control of Residual-Affected HCCI Engines.". ASME. J. Dyn. Sys., Meas., Control. 131(2).
- Solomatine, D., See, L., and Abrahart, R. (2008). "Data-Driven Modelling: Concepts, Approaches and Experiences", 17–30. Springer Berlin Heidelberg, Berlin, Heidelberg.
- Wong, K., Wong, P., Cheung, C., and Vong, C. (2013). "Modelling and optimisation of bio-diesel engine performance using advanced machine learning methods". Energy, 55, 519 – 528.
- Wong, P., Wong, K., Vong, C., and Cheung, C. (2015). "Modeling and optimization of bio-diesel engine performance using kernel-based extreme learning machine and cuckoo search". *Renewable Energy*, 74, 640 647.
- Zhang, S., Zhu, G., and Sun, Z. (2014). "A Control-Oriented Charge Mixing and Two-Zone HCCI Combustion Model". *IEEE Trans. on Veh Tech.*, 63(3), 1079–1090.